NANO LETTERS

2008
Vol. 8, No. 1
208−213

Reversible Switching among Three Adsorbate Configurations in a Single [2.2]Paracyclophane-Based Molecule

C. Silien,[†] N. Liu,[‡] and W. Ho*

Department of Physics and Astronomy and Department of Chemistry, University of California Irvine, California 92697-4575

J. B. Maddox and S. Mukamel

Department of Chemistry, University of California Irvine, California 92697-4575

B. Liu and G. C. Bazan

Department of Chemistry, University of California Santa Barbara, California 93106-9510

Received September 28, 2007; Revised Manuscript Received November 28, 2007

ABSTRACT

Single 4,7,12,15-tetrakis(4′-dimethylaminostyryl)[2.2]paracyclophane molecules adsorb on NiAl(110) in different configurations. When the symmetry axes of the molecules are properly oriented with respect to the surface lattice, three adsorbate states of different conductance can be reversibly induced and directly imaged with a scanning tunneling microscope. Couplings between tunneling electrons and adsorbate vibrational and electronic states are primarily responsible for the transformation. However, change from low to high conductance configuration can also be triggered by electric field in the junction.

In recent years, engineered molecules were built around the [2.2]paracyclophane skeleton to which various chemical groups, such as stilbene derivative, could be bonded.[1,2] Such molecules are interesting within the context of three-dimensional delocalization in organic chromophores and possess optical and electronic properties substantially different from their more common one- and two-dimensional counterparts.[3] To realize the optical properties of these molecules, it is desirable to understand their structural dependence, especially in view of the flexibility and possible distortion of the paracyclophane core. This paper reports a detailed study at the molecular level with the scanning tunneling microscope (STM) for 4,7,12,15-tetrakis(4′-dimethylaminostyryl)[2.2]paracyclophane (DMAS-PCP) molecules, which mimic the crossing of two oligo(phenylene-vinylene) molecular wires[4,5] [see Figure 1a]. The paracyclophane core holds the two units together with a well-defined orientation and facilitates strong through-space electronic interactions between the upper and lower units in addition to the through-bond interactions normally associated with π-conjugated backbones.

The reversible transitions between one high and two low conductance adsorbate states were observed in single DMAS-PCP molecules adsorbed on NiAl(110). Hysteretic properties in single molecules likely form the basis for the realization of nanoscale memories and logic devices.[6] Therefore, it is of prime interest to understand and control reversible changes in the electrical conductance of molecules. A multitude of phenomena have been observed on thin films and monolayers. They underline the importance of the interface with electrodes,[7] the molecule environment,[8,9] as well as the role of intrinsic molecular properties.[10−14] In particular, reversible conformation changes have been suggested to explain the variation of conductance observed with STM in single phenylene ethynylene oligomers embedded in alkanethiol monolayers[15] and in single isolated Zn-Etioporphyrin adsorbed on NiAl(110).[16] Reversible charging and discharging events of single Mg porphine molecules on oxidized NiAl(110) in a STM junction have also been observed and can be controlled with an external bias or laser field.[17] For DMAS-PCP, the hysteretic conversion among these different conductance states is achieved by controlling the electric current and field across the STM junction. The switching is

* To whom correspondence should be addressed. E-mail: wilsonho@uci.edu.

[†] Present address: University of St. Andrews, North Haugh, St. Andrews, KY16 9ST, U.K.

[‡] Present address: University of Alberta, Edmonton, T6G 2G7, Alberta, Canada.

10.1021/nl072493c CCC: $40.75
Published on Web 12/13/2007

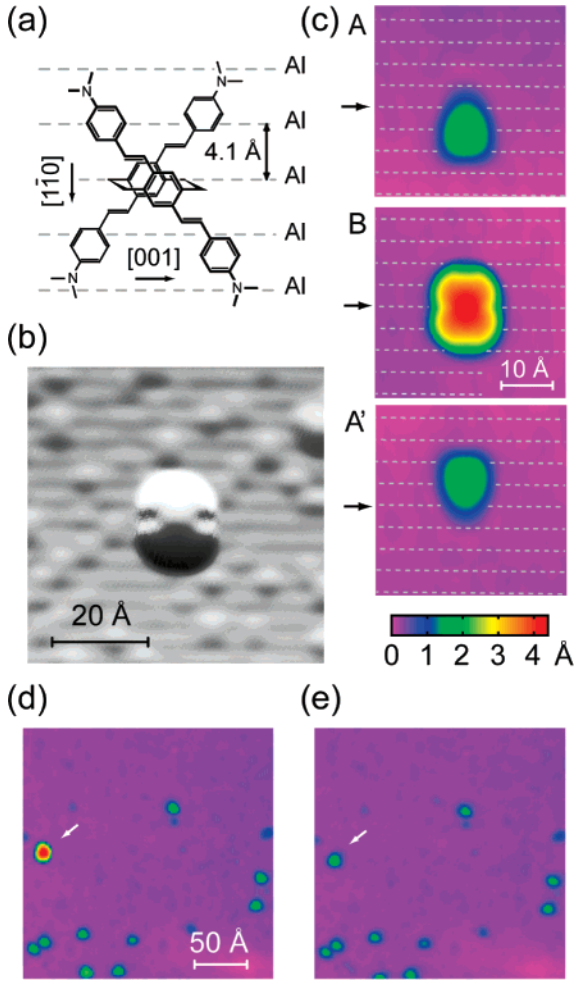

Figure 1. (a) Schematic representation of the DMAS-PCP molecule superimposed on the Al rows of the NiAl(110) surface lattice. (b) Contrast-enhanced (differentiated from the top) STM topography of a single DMAS-PCP on NiAl(110). The image was recorded with a current of 0.1 nA and the sample bias set at 1.75 V. (c) STM topographies of the same molecule as in panel b, all acquired with 0.1 nA and 0.36 V, before (B) and after (A and A′) controlled modification (see text for details). Dashed lines represent the Al rows of the surface lattice, and the arrows indicate the row over which the molecule (B) shown in panel c is symmetrically positioned. (d) STM image recorded at 0.1 nA and 0.25 V showing one molecule in the B state (see arrow) and 9 molecules in the A (A′) state that cannot be converted into B. (e) All molecules in the A (A′) configuration, after locally induced transformation of the molecule marked by the arrow.

only realized for one adsorption geometry on NiAl(110) suggesting that specific adsorbate−substrate interactions are involved. It was possible with the STM to directly image the three molecular configurations.

The experiments were accomplished with a homemade ultrahigh vacuum (UHV) STM based on a previously detailed design.[18] All the measurements were carried out at 11 K and pressure lower than 3×10^{-11} Torr. We used silver tips prepared by chemical etching and annealing in UHV.[19] The NiAl(110) surface was cleaned by repeated Ne^+ sputtering and annealing (∼1200 K) cycles. The DMAS-PCP was synthesized according to a procedure published elsewhere.[20] The molecules were evaporated in UHV from a heated alumina crucible onto the NiAl surface kept at 11 K.

Single DMAS-PCP molecules were first localized and identified as large protrusions by recording STM topographies with the sample bias set above 1.0 V. This high conductance state appears as depicted in the contrast-enhanced image shown in Figure 1b, which was recorded with a current of 0.1 nA and the sample bias set at 1.75 V. The image reveals some molecular structural details, as well as the molecule orientation and position with respect to the NiAl(110) surface lattice, because the Al rows, separated by 4.1 Å,[21] are also resolved. DMAS-PCP is visualized as a protrusion with 2-fold symmetry centered on one Al row. Two symmetric dips are detected on the edges of the molecules that lead us to conclude that one C_2 axis of DMAS-PCP is aligned parallel to the Al row, as pictured in Figure 1a. Given that all four dimethylaminostyryl groups are imaged similarly, we expect some molecular deformations.

An image of the same molecule recorded at 0.36 V (0.1 nA) and labeled B is shown in Figure 1c. Dashed lines mark the Al rows, since they are not visible for such voltage and color palette. The application of bias pulses reversibly modified the adsorbate configuration. When the polarity of the bias sample is temporarily reversed and set over a well-defined negative threshold, two symmetric, but otherwise identical, molecular states of low conductance are possible. These configurations, labeled A and A′ in Figure 1c, were acquired with the sample bias at 0.36 V and a current of 0.1 nA. The states A and A′ possess only a single mirror plane. They are realized depending on the precise tip location over B when applying the negative bias pulse: positioning the tip above (below) the central Al row leads to the conversion of B into A (A′). A temporary increase of the bias over a well-defined positive value causes states A and A′ to adopt again the high conductance state B. Fully reversible changes in the conductance of DMAS-PCP on NiAl(110) are therefore easily achieved and observed. STM offers spatial resolution for studying single molecules on surfaces that is difficult to match with other techniques. Because the topographic images reflect the electronic structure of the adsorbed molecules, it is sometimes difficult to determine their adsorption geometry. This is the case for DMAS-PCP in the A or A′ configuration. However, the reversibility of the transitions and the mirror symmetry of A and A′ indicate that the molecule is chemically unaltered during the process and that constrained molecular distortions of the paracyclophane and aminostyryl groups are involved, leading to the teardrop shapes shown in Figure 1c.

Imaging larger areas of the sample reveals that only a small amount (∼10%) of adsorbed molecules exhibit the reversible behavior (Figure 1d,e). Most of the molecules are not influenced by the bias. They have the same shape and apparent height as those of A albeit with different orientations on the substrate. All the molecules that undergo conversion are systematically oriented on the surface with one of their C_2 axes parallel to the Al rows. Because molecules in the configuration B are not observed on Cu(111) and Al_2O_3/NiAl(110), the precise orientation of DMAS-PCP on NiAl(110) detailed in Figure 1a is essential for stabilizing

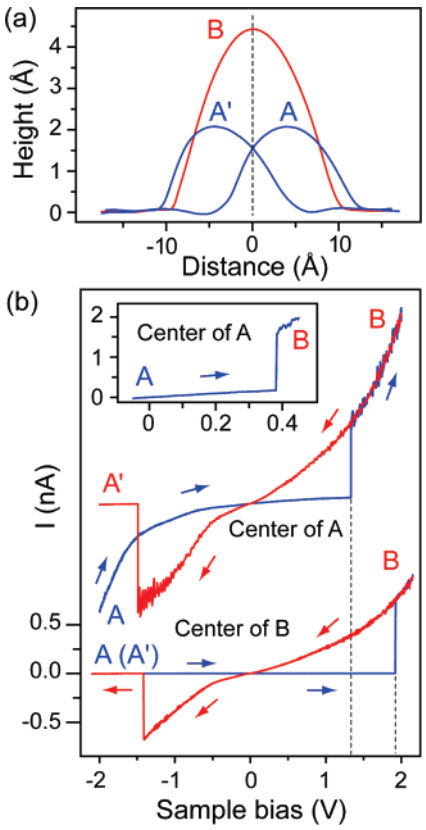

Figure 2. (a) Topographic profiles measured across the DMAS-PCP molecule and perpendicular to the Al rows on all the three images (A, A′, and B) shown in Figure 1c. (b) *I*(V) curves recorded by increasing and decreasing the sample bias (0.33 V/s) after positioning the tip and disabling the feedback loop. The bottom curves were recorded with the tip positioned at the center of B (0.62 nA at 1.75 V). The upper curves were acquired with the tip at the center of A (0.63 nA at −1.75 V). The labels indicate the states realized when ramping up and down the sample bias. The inset shows an *I*(V) curve measured (0.39 V/s) on a different molecule with the tip centered on A (0.1 nA at 0.20 V). The axes are presented with the same units as in the main graph.

both A and B configurations and allowing the hysteretic switching. Misorientation with respect to the NiAl(110) surface prevents DMAS-PCP to assume the state of high conductance B.

The mechanisms involved in the change of configurations of DMAS-PCP on NiAl(110) are determined by measuring the thresholds for transformation and their dependence on the tunneling current and the electric field under the STM tip. Figure 2a shows the variations of the tip height when scanning over the center of the molecule, presented in Figure 1, along the [1$\bar{1}$0] direction perpendicular to the Al rows. A large difference in conductance is observed between B and A (A′). Therefore, the conversions can be detected through *I*(V) measurements, and the switching threshold values can be easily determined. Three datasets are presented in Figure 2b. The bottom curves were acquired with the tip at the center of B and the tunneling gap set at 0.62 nA for 1.75 V. Because the bias is ramped below −2.0 V prior to recording the current, the initial molecular configuration is either A or A′, depending on asymmetries in the tip. The current is finally recorded while raising and decreasing the bias at a rate of 0.33 V/s. During the voltage increase, a 3 to 4 orders of magnitude rise in the current is readily detected at 1.85 ± 0.04 V. Such an increase indicates that the A (A′) molecule adopts the configuration of larger conductance B. Upon reducing the bias below −1.41 ± 0.04 V, the molecule changes back into A (A′), indicated by the abrupt decrease in the tunneling current. The transformation can be repeated virtually indefinitely.[22]

The second set of *I*(V) curves in Figure 2b was recorded by initially changing B into A, centering the tip over A, and adjusting the tunneling gap with a negative bias (0.63 nA for −1.75 V). Ramping up and down the bias eventually induces the transformation from A to B and B to A′. In the inset of Figure 2b, we show an *I*(V) curve recorded over another DMAS-PCP with the tip set at 0.1 nA for 0.20 V and centered on A prior to measurement (0.39 V/s). For such a reduced tip height, the conversion into B is detected for a bias as low as 0.41 ± 0.04 V. Afterward, the molecule was successfully changed back into A by using a greater tip height to avoid large currents, which would induce permanent changes in the molecule.

A significant difference in the positive bias required to transform A or A′ into B is thus observed between the three sets of *I*(V) curves. From Figure 2b, the current at 0.25 V bias are respectively 0.00012, 0.018, and 0.13 nA for the lower and upper sets and for the inset, so that both the amount of tunneling electrons and the electric field applied on the molecule are different. Nevertheless, for the negative threshold corresponding to the transformation of B into A′ or A, only a moderate variation is found in the data sets. To disentangle the roles of the current and the electric field and highlight the mechanisms for configuration change in DMAS-PCP on NiAl(110), the thresholds for transformation are measured as a function of the lateral distance from the center of A and B. Indeed, when moving the tip apex laterally away from the DMAS-PCP, the current flowing through the molecule should decrease exponentially. The magnitude of the electric field at the molecule would be reduced more gradually as a power law, after an initial decrease corresponding to the apex displacement. Thus, it is possible to discriminate between the two types of excitation.

For these measurements, the tip was positioned with the set point at 0.1 nA and 0.25 V. A 10 s constant-voltage pulse was applied with the feedback loop disabled. A change in the molecule configuration was verified by recording a topographic image at 0.25 V. The procedure was repeated with an incrementally higher voltage pulse until the conversion was observed. The plots of the transformation voltage as a function of the tip position along the direction of the Al rows are shown in Figure 3. To change A into B, the bias must be raised over ∼0.37 V when the tip is located over a DMAS-PCP molecule (Figure 3a). This value could not be reduced by increasing the pulse duration or reducing the tip height by adjusting the tunneling set point. Away from the molecule, the magnitude of the threshold increases drastically from ∼ 0.37 V at 6.7 Å to ∼ 1.8 V at 13.5 Å. However, the transformation remains achievable at large distance and the threshold, now above 1.8 V, appears saturated and rises only

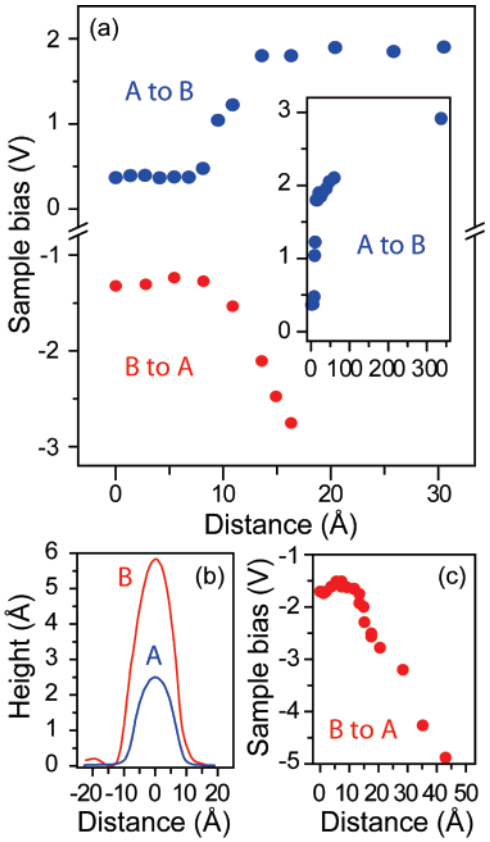

Figure 3. (a) Voltage pulses (10 s) required to transform A to B and B to A as a function of the lateral distance from the center of A and B, respectively. The configuration changes were obtained with the tunneling gap set at 0.1 nA for 0.25 V and verified by topographic measurements. The inset displays the threshold for changing A to B for larger tip-to-molecule distances. The axes are presented with the same units as in the main graph. (b) Topographic profiles of DMAS-PCP recorded with 0.1 nA and 1.75 V for B and A along the direction of the Al rows. (c) Thresholds for the transformation of B to A acquired with the tunneling gap set at 0.1 nA for 0.25 V. Voltage pulses (30 s) more negative than −3.0 V were attempted even though they led to significant modifications of the tip apex.

gradually with a moderate slope (see inset). The conversion could be induced as far as 337 Å away of the molecule for biases as low as 2.9 V. We did not try biases above 3.0 V.

For the conversion of B into A, we determined that the negative bias must be over ∼ −1.25 V when the tip is positioned over the molecule. This threshold increases rapidly when the tip is moved farther than 8.2 Å from the center of B. Biases over −3.0 V were not attempted in this data set because they modify the tip configuration and compromise the coherence of the results. Nevertheless, in a separate experiment, the threshold was found to increase quickly if the tip is further moved away: values below −4.9 V were necessary at 44 Å from the center of B (see Figure 3c).

The experimental observations for DMAS-PCP on NiAl(110) are explained below by considering that both the electric field and the tunneling current can initiate the conversion of A (A′) into B, while only the tunneling electrons induces the reverse transformation. Several published reports have already highlighted possible couplings between the adsorbates and the tunneling electrons. For example, coupling of tunneling electrons with vibrational modes of acetylene can induce its rotation on Cu(100),[23] oxygen can be desorbed from Pt(111) when exposed to the STM current,[24] and Zn−etioporphyrin on NiAl(110) can be reversibly modified when electrons tunnel into specific molecular orbitals.[16] For DMAS-PCP, when the tip is over A (A′) the ∼ 0.37 V threshold (Figure 3a) value coincides with the energy of CH stretch vibrations. It seems reasonable that the coupling between the tunneling electrons and the vibrational modes triggers the conversion to B. The opening of an inelastic conductance channel at this bias has indeed been observed in a separate experiment, indicating the existence of effective coupling between tunneling electrons and CH stretch vibrations.[25] On the other hand, when the tip is away from the molecule, the moderate slope for the thresholds and the large distance over which the transition to B can be realized suggest that the electric field is triggering the conversion. DMAS-PCP does not exhibit a dipole moment prior to deposition. However, it is significant to note that chromophores built on [2.2]paracyclophane are more polarizable than their standard oligo(phenylenevinylene) counterparts[26] and that the large change in the density of states (Figure 1c) when the molecule is transformed into A or A′ could induce a dipole. The coupling between the electric field and dipole moment would provide the necessary energy to overcome the barrier for transforming A into B at large tip-molecule distance where the couplings between the tunneling current and adsorbate are negligible.

The large variation in threshold for converting A to B, measured on the three sets of I(V) curves presented in Figure 2b, supports the possibility that both tunneling electrons and electric field trigger the conversion when the tip apex is positioned over the DMAS-PCP. Indeed, when the current flowing through the molecule is weak (lower dataset in Figure 2b), the threshold is 1.85 V, which is consistent with a conversion provoked by the electric field. On the other hand, when the current flowing into A is much larger (inset in Figure 2b), the transformation bias is 0.4 V, which is compatible with a substantial increase in the coupling of tunneling electrons with the vibrational modes. For the intermediate tunneling condition in our experiment (see upper data sets in Figure 2b), the averaged onset is 1.13 ± 0.19 V. At a given bias, a reduction of the tip height is responsible for an increase of the electric field, which could be responsible for the change of adsorbate configuration at bias lower than ∼1.8 V. However, although the current is lower, the electrons should still be able to initiate the conversion into B while the bias is above 0.37 V. The threshold for conversion of A (A′) clearly depends on the magnitude of the current. However, the electric field is able to trigger the conversion when the current is negligible. Appropriate choices of the tip location and height allow us to favor one mechanism over another to induce the conversion of A into B.

Unlike for the transformation of A into B, a saturation of the voltage at large distance for the conversion of B into A (A′) was not observed (Figure 3a,c). Thus, the electric field alone is not able to modify the molecular state and that the tunneling current through the DMAS-PCP is responsible for

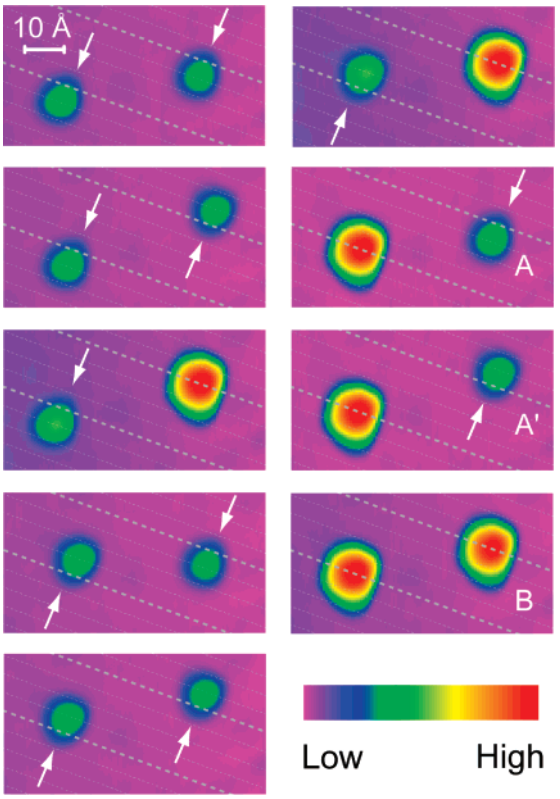

Figure 4. Sequence of STM topographies of a pair of isolated DMAS-PCP on NiAl(110). All images were recorded with a current of 0.1 nA and the sample bias set at 0.25 V. Dotted lines indicate the location of the Al rows. Thicker traces are used for the rows supporting the two DMAS-PCP molecules. All nine possible configurations of the pair were realized by applying appropriate bias pulses over the molecules. The same color palette is used for all nine images.

the switching. However, the negative threshold for transformation is too large to be related to the excitation of molecular vibrations and indicates that one or several filled electronic states below ~ -1.25 V are involved. Little variations in the onset for conversion are observed when using different tip heights and different apexes. Even though the electric field alone is unable to trigger the reverse conversion, we cannot exclude that its magnitude modifies the threshold. While the tunnel current should be confined to atomic dimensions, the transformation into A remains possible at moderately large distance (44 Å) if the voltage is set over −4.9 V. This suggests that secondary processes involving the propagation of electrons through surface states induce the change of molecular state. Such an argument has been used previously to justify the long range (∼100 Å) dissociation of O_2 on Pt(111) induced by electrons tunneling at 1.0 V.[24]

For low voltages, the reversible transformation of DMAS-PCP on NiAl(110), strictly by tunneling electrons coupling with adsorbate vibrational and electronic states, enables control of high-density devices because the current is concentrated within a small area directly underneath the tip apex. Such high-precision control is not easily achieved if electric fields are the prevailing perturbations, because the field is not confined. This is illustrated in Figure 4, where we show a sequence of topographical images of a pair of DMAS-PCP molecules separated by 35 Å (center to center distance) and whose respective configurations were modified independently and predictably. All the nine possible situations were reproducibly achieved, by applying appropriate voltage pulses on the center or edges of each molecule, and measured with 0.1 nA and 0.25 V.

In conclusion, [2.2]paracyclophane-based single molecules on NiAl(110) have been investigated at molecular resolution with the STM. When the symmetry axes of the molecules are properly aligned with the surface lattice, the adsorbed molecules can be reversibly transformed between three configurations that have been imaged in details. Two configurations with reduced symmetry (A, A′) exhibit conductances significantly lower than the third one (B). Molecules are trapped in configuration of low conductance if they are misoriented with respect to the substrate. The mechanisms for transformation have been investigated. It was determined that couplings between the tunneling electrons and adsorbate vibrational and electronic states are primarily responsible for the hysteretic behavior. However, the transformation from A (A′) to B can also be triggered by the electric field when the current flowing through the molecule is negligible. The mirror symmetry of the low conductance states with respect to the Al row on which the molecule is centered suggests that the paracyclophane group plays an important role in the transformation and stabilization of the adsorbate configurations. The present work highlights the possibility to directly image and induce reversible changes in the adsorbate configurations of adsorbed [2,2]paracyclophane-based molecules thus providing insight into the effects of the possible distortion of the paracyclophane core on their electronic properties.

Acknowledgment. This work has been supported by the National Science Foundation, Chemical Bonding Center, Grant CHE-0533162. In addition, S.M. and G.C.B. gratefully acknowledge the support of NSF NIRT, and W.H. acknowledges the Air Force Office of Scientific Research, Grant FA9550-04-1-0181. At the time of the research, C.S. was a Scientific Research Worker of the Belgian National Fund for Scientific Research (FNRS).

References

(1) Bartholomew, G. P.; Bazan, G. C. *Synthesis* **2002**, *9*, 1245−1255.
(2) Ruseckas, A.; Namdas, E. B.; Lee, J. Y.; Mukamel, S.; Wang, S.; Bazan, G. C.; Sundstrom, V. *J. Phys. Chem. A* **2003**, *107*, 8029−8034.
(3) Bartholomew, G. P.; Ledoux, I.; Mukamel, S.; Bazan, G. C.; Zyss, J. *J. Am. Chem. Soc.* **2002**, *124*, 13480−13485.
(4) Seferos, D. S.; Blum, A. S.; Kushmerick, J. G.; Bazan, G. C. *J. Am. Chem. Soc.* **2006**, *128*, 11260−11267.
(5) Seferos, D. S.; Trammell, S. A; Bazan, G. C.; Kushmerick, J. G. *Proc. Nat. Acad. Sci. U.S.A.* **2005**, *102*, 8821−8825.
(6) Wada, Y. *Proc. IEEE* **2001**, *89*, 1147−1171.
(7) Stewart, D. R.; Ohlberg, D. A. A.; Beck, P. A; Chen, Y.; Williams, R. S.; Jeppesen, J. O.; Nielsen, K. A.; Stoddart, J. F. *Nano Lett.* **2004**, *4*, 133−136.
(8) Lau, C. N.; Stewart, D. R.; Williams, R. S.; Bockrath, M. *Nano Lett.* **2004**, *4*, 569−572.
(9) Gao, H. J.; Sohlberg, K.; Xue, Z. Q.; Chen, H. Y.; Hou, S. M.; Ma, L. P.; Fang, X. W.; Pang, S. J.; Pennycook, S. J. *Phys. Rev. Lett.* **2000**, *84*, 1780−1783.
(10) Collier, C. P.; Mattersteig, G.; Wong, E. W.; Luo, Y.; Beverly, K.; Sampaio, J.; Raymo, F. M.; Stoddart, J. F.; Heath, J. R. *Science* **2000**, *289*, 1172−1175.

(11) Pease, R.; Jeppesen, J. O.; Stoddart, J. F.; Luo, Y.; Collier, C. P.; Heath, J. R. *Acc. Chem. Res.* **2001**, *34*, 433−444.
(12) Gittins, D. I.; Bethell, D.; Schiffrin, D. J.; Nichols, R. J. *Nature* **2000**, *408*, 67−69.
(13) Reed, M. A; Chen, J.; Rawlett, A. M.; Price, D. W.; Tour, J. M. *Appl. Phys. Lett.* **2001**, *78*, 3735−3737.
(14) Bandyopadhyay, A.; Pal, A. J. *Appl. Phys. Lett.* **2004**, *84*, 999−1001.
(15) Donhauser, Z. J.; Mantooth, B. A; Kelly, K. F.; Bumm, L. A.; Monnell, J. D.; Stapelton, J. J.; Price, D. W., Jr.; Rawlett, A. M.; Allara, D. L.; Tour, J. M.; Weiss, P. S. *Science* **2001**, *292*, 2303−2307.
(16) Qiu, X. H.; Nazin, G. V.; Ho, W. *Phys. Rev. Lett.* **2004**, *93*, 196806.
(17) Wu, S. W.; Ogawa, N.; Ho, W. *Science* **2006**, *312*, 1362−1365.
(18) Stipe, B. C.; Rezaei, M. A.; Ho, W. *Rev. Sci. Instrum.* **1999**, *70*, 137−143.
(19) Liu, N.; Pradhan, N. A.; Ho, W. *J. Chem. Phys.* **2004**, *120*, 11371−11375.
(20) Bartholomew, G. P.; Bazan, G. C. *J. Am. Chem. Soc.* **2002**, *124*, 5183−5196.
(21) Nilius, N.; Wallis, T. M.; Persson, M.; Ho, W. *Phys. Rev. Lett.* **2003**, *90*, 196103.
(22) The molecule remains unaltered even after changing over 920 times its configuration from B to A (or A′) and back to B.
(23) Stipe, B. C.; Rezaei, M. A.; Ho, W. *Phys. Rev. Lett.* **1998**, *81*, 1263−1266.
(24) Stipe, B. C.; Rezeai, M. A.; Ho, W. *J. Chem. Phys.* **1997**, *107*, 6443−6447.
(25) The CH stretch vibration is observed at 365 mV by inelastic electron tunneling spectroscopy (IETS) with the STM. In addition, four other vibrational modes (25, 40, 60, and 179 mV) are resolved in the STM-IETS spectra.
(26) Hong, J. W.; Woo, H. Y.; Liu, B.; Bazan, G. C. *J. Am. Chem. Soc.* **2005**, *127*, 7435−7443.

NL072493C